Eur Radiol (2007) 17: 259–264
DOI 10.1007/s00330-006-0224-3

K.-H. Herrmann
S. Wurdinger
D. R. Fischer
I. Krumbein
M. Schmitt
G. Hermosillo
K. Chaudhuri
A. Krishnan
M. Salganicoff
W. A. Kaiser
J. R. Reichenbach

Application and assessment of a robust elastic motion correction algorithm to dynamic MRI

Received: 28 April 2005
Accepted: 23 February 2006
Published online: 13 April 2006

K.-H. Herrmann (✉) ·
J. R. Reichenbach
Medical Physics Group,
Institute for Diagnostic and
Interventional Radiology,
Friedrich-Schiller-Universität Jena,
Philosophenweg 3,
07743 Jena, Germany
e-mail: Karl-Heinz.Herrmann@med.uni-jena.de
Tel.: +49-3641-935365
Fax: +49-3641-936767

S. Wurdinger · D. R. Fischer ·
I. Krumbein · W. A. Kaiser
Institute for Diagnostic and
Interventional Radiology, Friedrich-Schiller-Universität Jena,
Erlanger Allee 101,
07747 Jena, Germany

M. Schmitt
Siemens Medical Solutions,
Erlangen, Germany

G. Hermosillo · K. Chaudhuri ·
A. Krishnan · M. Salganicoff
Siemens Computer Aided Diagnosis and Therapy,
Malvern, Pennsylvania, USA

Abstract The purpose of this study was to assess the performance of a new motion correction algorithm. Twenty-five dynamic MR mammography (MRM) data sets and 25 contrast-enhanced three-dimensional peripheral MR angiographic (MRA) data sets which were affected by patient motion of varying severeness were selected retrospectively from routine examinations. Anonymized data were registered by a new experimental elastic motion correction algorithm. The algorithm works by computing a similarity measure for the two volumes that takes into account expected signal changes due to the presence of a contrast agent while penalizing other signal changes caused by patient motion. A conjugate gradient method is used to find the best possible set of motion parameters that maximizes the similarity measures across the entire volume. Images before and after correction were visually evaluated and scored by experienced radiologists with respect to reduction of motion, improvement of image quality, disappearance of existing lesions or creation of artifactual lesions. It was found that the correction improves image quality (76% for MRM and 96% for MRA) and diagnosability (60% for MRM and 96% for MRA).

Keywords Motion correction · MR mammography · MR angiography · Motion artifacts · Registration

Introduction

Dynamic contrast-enhanced (CE) magnetic resonance imaging (MRI) is an important and valuable diagnostic tool, especially for the investigation of vessel and tissue status as is the case in MR mammography (MRM) or MR angiography (MRA). For the analysis of a dynamic CE MR study it is essential that no changes in the patient's position occur during the whole acquisition. However, this requirement is often not met and may thus affect interpretation of the images or even prevent accurate diagnosis [1, 2].

Regardless of the many efforts undertaken to reduce or suppress motion artifacts there remains quite a substantial number of examinations which suffer from motion induced artifacts. To take into account the highly non-linear elastic properties of human tissue (e.g., breast, muscle) several elastic deformation image registration algorithms have been published [3–8]. One of the dangers with elastic

algorithms, however, is that some parts of the original image might vanish because of overlays or singular distortion fields [9].

An additional problem encountered in CE dynamic MRI is the actual change of the image signal due to the presence of a contrast agent and any useful registration algorithm has to be robust against signal enhancing areas which may be highly localized but can also be — especially in MRM— multifocal, diffuse or even cover the whole breast. Simultaneously, the image registration has to preserve the signal changes due to a contrast agent. In the new algorithm this is taken into account by carefully adjusting the similarity measure.

The aim of the present study was to investigate the performance of a new experimental motion correction algorithm by applying it retrospectively to dynamic MRI data sets of patients who had undergone MRM or peripheral MRA.

Materials and methods

Patients

Twenty-five contrast-enhanced MRM data sets (patients' age range: 33–73 years) and 25 dynamic peripheral MRA data sets (age range: 49–84 years) affected by motion artifacts of varying severeness were retrospectively selected from routine examinations for further analysis. The medically indicated CE MRI examinations were conducted with informed consent by the patients. Selection of the data sets was based on the presence of visible motion artifacts in the images, regardless of the actual diagnosis. Data sets were selected from routine examinations during a time period of 3 months. The percentage of cases with visible motion artifacts was approximately 12% for MRM and 30% for MRA.

MR sequences

Dynamic MR mammography was performed by using a two-dimensional (2D) multislice, T_1 -weighted FLASH sequence on a 1.5 T scanner (Magnetom Symphony, Siemens Medical Solutions, Erlangen, Germany) and a double breast coil with the following scan parameters: T_R / T_E / α = 113 ms / 4.76 ms/80 °, matrix 384 × 384, $FoV = 350$ mm , slice thickness 3 mm, inter slice distance 10–30% of slice thickness depending on volume coverage requirements, GRAPPA partial parallel imaging acceleration factor 2, scan time 60 s. The dynamic contrast examination was performed with one native scan followed by a series of seven scans, one each minute, after CA injection.

The contrast enhanced peripheral angiography data were acquired with a 3D FLASH sequence on a 1.5 T scanner (Magnetom Symphony or Sonata, Siemens Medical Solutions, Erlangen, Germany). Typical parameters were T_R / T_E / $\alpha = 4$ ms / 1.5 ms/40°, slice thickness 1 mm matrix of 384–512 and 80–104 partitions, GRAPPA acceleration factor 3 and FoV of up to 500 mm Two data sets were acquired, one native and one after administration of a contrast agent.

Motion correction algorithm

An experimental version of a new elastic motion correction algorithm, developed by Siemens Medical Solutions (Malvern, Penn., USA), was applied to the data. The main component in the algorithm is the estimation of the compensating deformation between a reference and a floating image for a given resolution level. This is done by maximizing a similarity measure S between the two images, based on the local cross correlation of corresponding regions around each point. The local cross correlation L_{CC} between the 3D images I_1 and I_2 is defined as:

$$S = \int_{\Omega} L_{CC}(x)\,dx = \int \frac{v_{1,2}(x)^2}{v_1(x)v_2(x)}\,dx \tag{1}$$

where Ω is the volume coverage of the MR data, $v_{1,2}(x)$ is the covariance and $v_1(x)$, $v_2(x)$ are the variances of the intensities I_1 and I_2 in a Gaussian neighborhood centered on position x. The first order variation of L_{CC} is well defined and defines a gradient given by:

$$\nabla L_{CC} = f_{CC}\big(I(x), x\big)\ \nabla I_2(x) \tag{2}$$

where the intensity $I(x)$ at point x contains the pair of values (intensities):

$$I(x) \equiv [I_1(x), I_2(x)] \tag{3}$$

and f_{CC} is the derivative of the local cross correlation with respect to the intensity variable. The localization is realized by a convolution of a Gaussian kernel with all spatially dependent variables. The cross correlation is robust to local changes in brightness and contrast within its local region and is therefore well adapted to perfusion sequences. The size of the local region is chosen to be approximately the same as the smallest expected detectable lesion.

The goal of the motion correction is then to find a deformation ϕ that maximizes the similarity measure S between I_1 and $I_2 \circ \phi(x)$. Here $\circ$ denotes a composition of functions, i.e. $(I_2 \circ \phi)(x) \equiv I_2\big(\phi(x)\big)$. With each deformation ϕ a displacement field U is associated such that $\phi = id + U$ (id is identity). The motion correction

algorithm tries to find a displacement field (a volume of three dimensional vectors) that makes $S\big(I_1, I_2 \circ \phi(x)\big)$ maximal. The warping of the image, i.e. calculation of $(I_2 \circ \phi)(x)$, requires tri-linear interpolation at each voxel of the image to be warped.

The algorithm uses a Fletcher-Reeves conjugate gradient (CG) optimization with line search [10] to find the final deformation ϕ, which is explicitly obtained by a composition of small invertible deformations. The displacement v_k corresponding to each small deformation is the regularized gradient of the similarity measure S between I_1 and $I_2 \circ \phi$. Starting from the deformation $\phi_1 = id$ the CG optimization is carried out for $k = 1, \ldots, n$:

$$v_k = G_\sigma \star \nabla S\big(I_1, I_2 \circ \phi_k(x)\big) \tag{4}$$

$$\phi_{k+1} = \phi_k \circ (id + \varepsilon_k v_k) \tag{5}$$

where the operator $G_\sigma\star$ denotes convolution by a Gaussian kernel and ∇S denotes the gradient of S with respect to ϕ. At each step, the invertibility of $id + \varepsilon_k v_k$ is guaranteed by the smoothness of v_k, and by choosing ε_k such that the maximum displacement over the image domain is less than one voxel.

This composition of small displacements ensures that the final deformation will not become singular and thereby provides a warranty that all structures in the uncorrected image will still be present after correction. This represents the major advantage in comparison to previously published methods which do not provide such a warranty. To speed up calculation a multi-resolution pyramid is used for a quick recovery of large displacements. More details can be found in [11].

Evaluation

To assess algorithm performance, the anonymized MR data were analyzed and subtraction images were calculated. Since routine diagnosis of peripheral MRA includes maximum intensity projections (MIP) of the subtracted images, MIPs were calculated for the MRA data.

The typical duration for correcting a complete dynamic breast MRI examination with a matrix of 384×384, 33 slices and all eight acquired volumes was 1 min. Depending on the number of slices and resolution, motion correction of the MRA data required typically 1–3 min.

All MR images were visually inspected and evaluated retrospectively by two experienced and highly trained radiologists in consensus. Based on the uncorrected subtraction images the motion induced artifacts were visually classified into two classes “moderate” and “severe”.

To evaluate MRM data, the uncorrected (UC) and corrected (CC) images were compared at 1, 2 and 7 min after contrast agent administration and rated on a “better—same — worse” scale with respect to improvement of image quality and diagnosability. Careful attention was given to the possible disappearance of existing lesions or creation of artifactual lesions. Together with the uncorrected and corrected subtraction images the original, unsubtracted images and the T_2 -weighted images were provided to the radiologist as in routine diagnosis.

For the evaluation of the 3D MRA data uncorrected and corrected images were compared. The algorithm performance was also rated on a “better—same—worse” scale and careful attention was given to the visibility of tiny vessels.

Results

The results of the evaluation are summarized in Table 1. For both applications, i.e., MRA and MRM, the algorithm was successful in most cases. Some of the results are described in greater detail below.

MRM

Although many dynamic breast MRI examinations reveal some minimal motion artifacts, most of them do not affect diagnosis. The correction algorithm unavoidably causes light blurring due to the interpolation of the data set and does not improve image quality necessarily for such

Table 1 Summary of the radiological evaluation of the corrected MR data sets in comparison to the uncorrected images. Image quality was rated based on subjective impression and diagnostic usability was rated on clarity of lesions (MRM) or vessel delineation (MRA). The percent values are calculated separately for MRM and MRA and for each class of motion severeness

	Image quality			Diagnostic usability		
	Better	Same	Worse	Better	Same	Worse
Breast MRI						
Moderate motion	14 (78%)	1 (5.6%)	3 (17%)	11 (61%)	4 (22%)	3 (17%)
Severe motion	5 (72%)	1 (14%)	1 (14%)	4 (57%)	2 (29%)	1 (14%)
Peripheral Angiography						
Moderate motion	15 (94%)	0	1 (6%)	15 (94%)	1 (6%)	0
Severe motion	9 (100%)	0	0	9 (100%)	0	0

minimal motion artifacts. Therefore, we did not consider these artifacts in our study.

For moderate and severe motion artifacts, however, the algorithm improved image quality in most cases (19 better vs two the same, and four worse; see Table 1). The improvement of diagnostic usability was rated slightly less efficient (15 better vs six the same and three worse). Examples are shown in Figs. 1, 2.

One case, where the software facilitated diagnosis, is shown in Fig. 1. Although patient motion was not particularly strong, the resulting artifacts are severe (Fig. 1a), making the lesion almost invisible among other bright artifacts. In the corrected image (Fig. 1b), the lesion is well delineated and the artifacts are completely eliminated.

While the software was very helpful in most cases of motion artifacts, there were a few cases with suspicious areas after correction. The uncorrected image in Fig. 2a is strongly affected by patient motion. While the corrected image (Fig. 2b) shows improvement in most areas there is a light enhancement in the marked area (*arrow*). The unsubtracted original data (not shown) did not support any existence of this enhancement.

MRA

The algorithm performed very well on MRA data sets which were affected by motion (see Table 1). Most of the artifacts were completely removed in the MIPs. No additional subtraction artifacts were introduced in all but one case where a very light, diffuse artifact was generated. Figure 3 shows one example of an MRA of the upper leg and knee area with very severe motion artifacts. The uncorrected MIP (Fig. 3a) suffers from large, bright artifacts. In addition, it shows an anatomically plausible vena saphena magna ("vein"), implying that the contrast agent has already reached this venous vessel, which, however, is an erroneous result due to patient motion. The correction algorithm not only eliminates all the irritating artifacts at tissue boundaries (Fig. 3b) but also eliminates the fake CA signal of the vein while conserving the real CA signal of the arteries.

Figure 4 shows a MIP where a diagnostically relevant part of the image is affected. The stenosis of the arteria tibialis posterior is completely hidden by the band-like artifact in the uncorrected image (*left*), but clearly visible in the corrected image (*right*, see *arrow*).

Discussion

Data corruption resulting from patient motion can be a serious limitation in many MR examinations. Patient movement can lead to false enhancing regions, causing longer diagnostic reading times and less clear diagnoses. On the other hand, motion correction by registration can correct for artifacts and potentially eliminates the need for a second scan if patient movement is severe. Although several different techniques have been developed to correct for patient motion, each technique has specific capabilities and limitations.

Apart from non-image-based techniques, such as immobilization, and imaging methods at the time of the MRI examination, like navigator-based motion compensation or real time tracking, there is a growing number of publications on image based post-processing techniques to reduce motion artifacts.

One of the problems of correcting MR breast data is that breast tissue deforms in a non-rigid, non-linear manner and does not contain unambiguous internal landmarks. Although there have been several approaches to the problem of matching MR data of the breast [3–8, 12, 13], many degrees of freedom are required to perform these non-rigid elastic transformations which makes the registration problem more challenging and computationally more burdensome [3–5].

Our registration algorithm overcomes this limitation by working on a reduced set of parameters and efficiently computing a dense deformation map from these param-

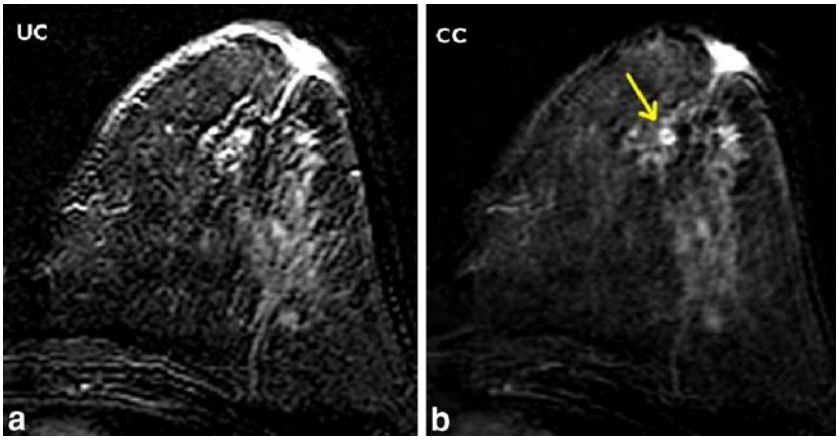

Fig. 1a, b MRM (2D) subtraction images of a female patient, aged 41 years. **a** The lesion is very difficult to detect in this uncorrected image among all artifacts. **b** The lesion is clearly visible after correction

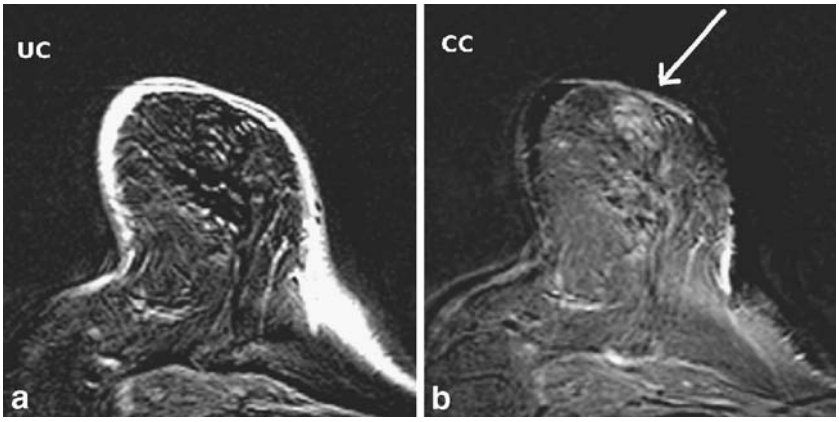

Fig. 2a, b MRM (2D) subtraction images of a female patient, aged 61 years. **a** The uncorrected image shows strong artifacts. **b** After correction: the artifacts are eliminated, but a suspicious patchy area (*arrow*) has been produced by the correction algorithm. There is no indication in the uncorrected images for signal enhancement in that area

eters. The algorithm ensures that the deformation map stays invertible, which is important to ensure that structures in the uncorrected image are not shrunk to a point in the corrected image at which they become invisible. Additionally, the new algorithm uses a robust similarity measure that avoids erroneous interpretation of signal enhancement due to contrast-agent intake as motion.

For dynamic MRM the software improved image quality. It also assisted and enabled successfully the diagnosis based on subtraction images in most cases. In none of the evaluated data sets was obscuration or disappearance of lesions observed after the correction. Nevertheless, it should be pointed out that only part of the data sets contained lesions and the algorithm should be validated further on pathological cases. Although the algorithm is very capable in correcting motion artifacts for focal lesions, it might prove more difficult to correct motion artifacts in the presence of diffuse contrast enhancements, as commonly seen in, for example, DCIS patients. As demonstrated in Fig. 2, light, diffuse enhancements can be created by the software. Therefore, further patient studies, especially with a diagnosis of DCIS or mastitis, are necessary.

For contrast-enhanced peripheral MRA the correction software was found to be highly useful as it substantially improved the subtraction images and the commonly used

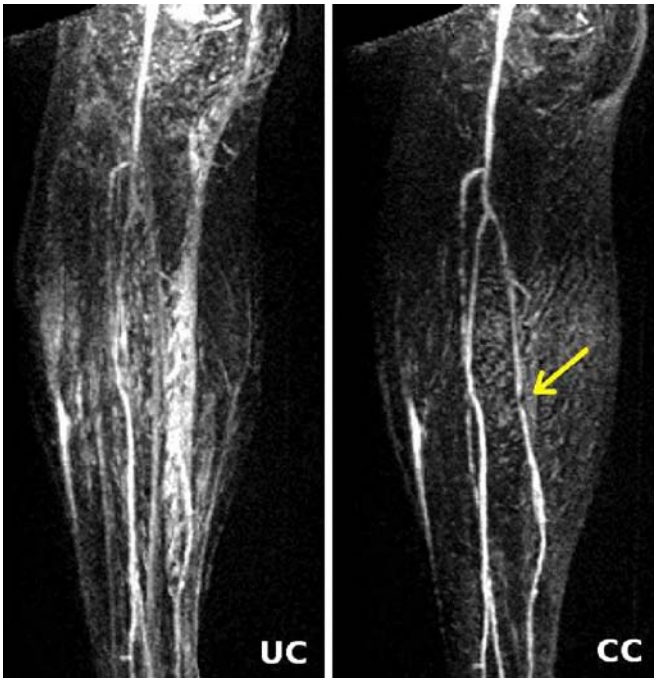

Fig. 4 Contrast-enhanced peripheral MR angiogram of a female patient, aged 64 years, with a stenosis of the right arteria tibialis posterior in the corrected MIP (right). The stenosis is not visible in the uncorrected images (left)

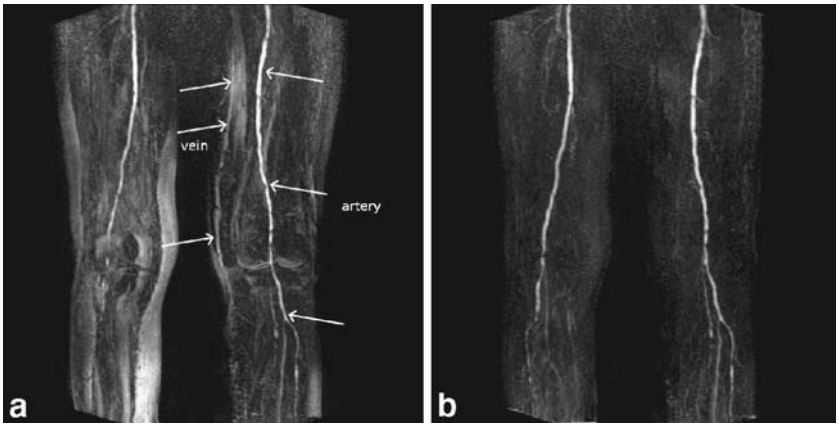

Fig. 3a, b Peripheral angiogram of the lower legs of a female patient, aged 84 years, with severe motion artifacts. **a** MIP image of the uncorrected data. Strong surface artifacts obscure large areas. The vena saphena magna (*arrows*) is displayed with erroneously "enhanced" signal. **b** MIP of the corrected data. All surface artifacts in **a** are removed and the vein is not visible in the MIP image. The arteries are not suppressed

MIPs. This shortens reading times of angiography images and data sets, and facilitates fast and accurate diagnosis.

In comparison, the correction algorithm performed better for MRA than for MRM. One of the reasons for this finding is the presence of easily identified internal landmarks (bones, fat, muscle boundaries) in MRA, which are missing in breast MRI. Furthermore, many breast MR exams show only very light motion artifacts. Since radiologists are well familiar with these artifacts, diagnosis is not hampered at all. On the other hand, even light artifacts can affect the quick survey of the vessel status and may make MIPs of MRA exams quite useless. Here, the algorithm helped to improve image quality even in cases with minor artifacts.

Conclusions

In summary, the proposed algorithm has been shown to improve the quality of subtracted MR images and computed data such as MIPs. Using the software may help to overcome the need for a second examination if patient movement has caused artifacts that obscure the images. In addition, the time required to read and analyze the data may be reduced, since many of the falsely enhancing areas were eliminated. The corrected images are not a replacement of the uncorrected images, but represent a valuable adjunct. Examining the corrected subtractions can help to detect otherwise possibly missed lesions (Fig. 1).

Due to its experimental status, the software was only provided for offline use; however, the motion correction for breast post processing is planned for full integration in the scanner software. Further optimization with respect to speed and display capabilities would allow to view side by side the original and the corrected images immediately after image reconstruction.

References

1. Heywang-Köbrunner SH, Viehweg P, Heinig A, Kächler C (1997) Contrast-enhanced MRI of the breast: accuracy, value, controversies, solutions. Eur J Radiol 24:94–108
2. Teifke A, Hlawatsch A, Beier T, Vomweg TW, Schadmand S, Schmidt M, Lehr HA, Thelen M (2002) Undetected malignancies of the breast: dynamic contrast-enhanced MR imaging at 1.0 T. Radiology 224:881–888
3. Fischer H, Otte M, Ehritt-Braun C, Laubenberger J, Hennig J (1999) Local elastic matching and pattern recognition in MR mammography. Int J Imaging Syst Technol 10:199–206
4. Rueckert D, Sonoda LI, Hayes C, Hill DLG, Leach MO, Hawkes DJ (1999) Non-rigid registration using free-form deformations: application to breast MR images. IEEE Trans Med Imaging 18:712–721
5. Lucht L, Knopp MV, Brix G (2000) Elastic matching of dynamic MR mammographic images. Magn Reson Med 43:9–16
6. Tanner C, Schnabel JA, Clarkson MJ, Rueckert D, Hill DLG, Hawkes DJ (2000) Volume and shape preservation of enhancing lesions when applying non-rigid registration to a time series of contrast enhancing MR breast images. In: Delp SL, DiGoia AM, Jaramaz B (eds) Lecture Notes in Computer Science, vol 1935 – Third Int. Conf. on Medical Image Computing and Computer-Assisted Intervention. Springer, Berlin Heidelberg New York, pp 327–337
7. Schnabel JA, Tanner C, Castellano-Smith AD, Degenhard A, Leach MO, Hose DR, Hill DL, Hawkes DJ (2003) Validation of nonrigid image registration using finite-element methods: application to breast MR images. IEEE Trans Med Imaging 22:238–247
8. Lu W, Chen ML, Olivera GH, Ruchala KJ, Mackie TR (2004) Fast free-form deformable registration via calculus of variations. Phys Med Biol 49:3067–3087
9. He J, Christensen GE (2003) Large deformation inverse consistent elastic image registration. Inf Process Med Imaging 18:438–449
10. Press William H, Teukolsky Saul A, Vetterling William T, Flannery Brian P (1988) Numerical recipes in C. Cambridge University Press, New York
11. Hermosillo Gerardo (2002) Variational methods for multimodal image matching. PhD thesis, Institut National de Recherche en Informatique et en Automatique (INRIA), Nice
12. Reichenbach JR, Hopfe J, Bellemann ME, Kaiser WA (2002) Development and validation of an algorithm for registration of serial 3D MR breast data sets. MAGMA 14:249–257
13. Rohlfing T, Maurer CR Jr, Bluemke DA, Jacobs MA (2003) Volume-preserving nonrigid registration of MR breast images using free-form deformation with an incompressibility constraint. IEEE Trans Med Imaging 22:730–741